Supporting Information to

CdSe@CdS Dot@Platelet Nanocrystals: Controlled Epitaxy, Mono-Exponential Decay of Two-Dimensional Exciton, and Non-Blinking Photoluminescence of Single Nanocrystal

Yonghong Wang†, Chaodan Pu†, Hairui Lei, Haiyan Qin, Xiaogang Peng*

Center for Chemistry of Novel & High-Performance Materials, Department of Chemistry, Zhejiang University, Hangzhou 310027, China.

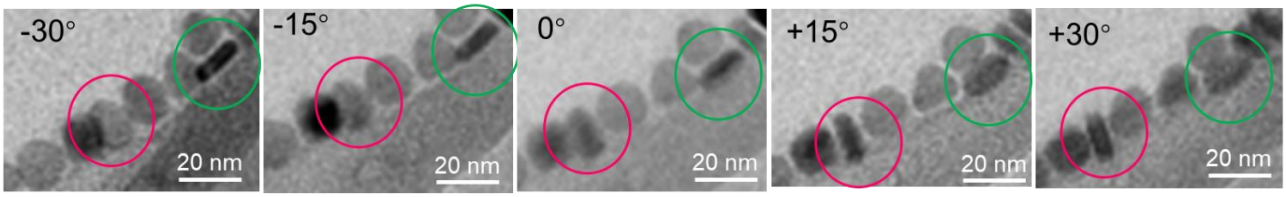

Figure S1. TEM images of the CdSe@CdS dot@platelet 2D nanocrystals obtained during rotating the specimen at different angles around an axis perpendicular to the electron beam. Two representative nanocrystals are cycled in each image for tracking purpose.

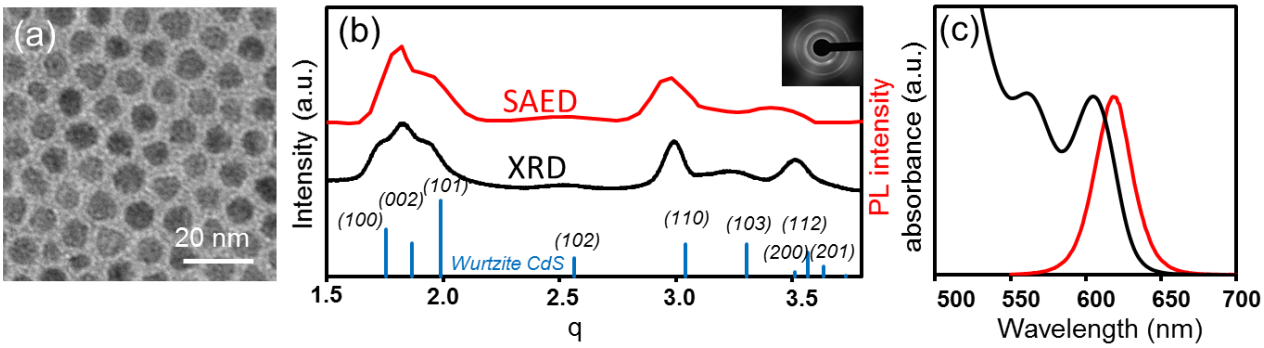

Figure S2. (a) TEM image of spheroidal CdSe/CdS core/shell nanocrystals synthesized with the Cd to S precursor ratio being greater than 1 to 1. (b) XRD pattern and integrated intensity profile from SAED pattern of the spheroidal CdSe/CdS core/shell nanocrystals. Inset: The SAED pattern of the sample. In comparison to the 2D nanocrystals, the XRD an SAED patterns are similar to each other for the spheroidal ones, indicating no preferential orientation of the nanocrystals in (a). (c) UV-Vis and PL spectra of the sample.

	d_{CdSe}	d_{CdS}	δ_{bulk}	$d_{experimental}$	$\delta_{experimental}$
(100)	0.3731	0.3578	4.1%	0.3593	3.7%
(002)	0.3512	0.3367	4.1%	0.3406	3.0%
(110)	0.2154	0.2066	4.1%	0.2082	3.3%

Table S1. Lattice compression of CdSe core by the CdS shells along and perpendicular to the c-axis of wurtzite lattice (thickness direction). The lattice constants are obtained from PDF card #65-3415for bulk wurtzite CdSe and #65-3414 for bulk wurtzite CdS.

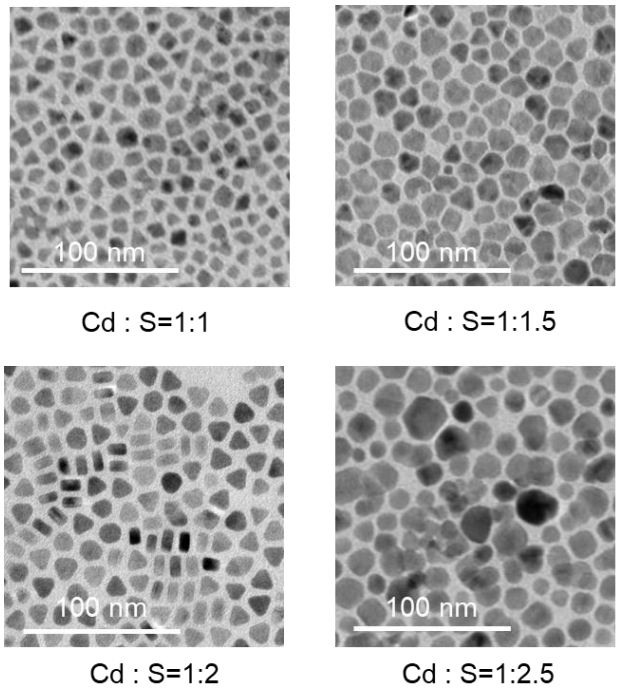

Figure S3. TEM images of the CdSe/CdS core/shell nanocrystals synthesized with different Cd to S precursor ratio (Cd:S). When the Cd to S precursor ratio is too low, such as being 1 : 2.5, aggregation of the nanocrystals becomes hard to prevent.

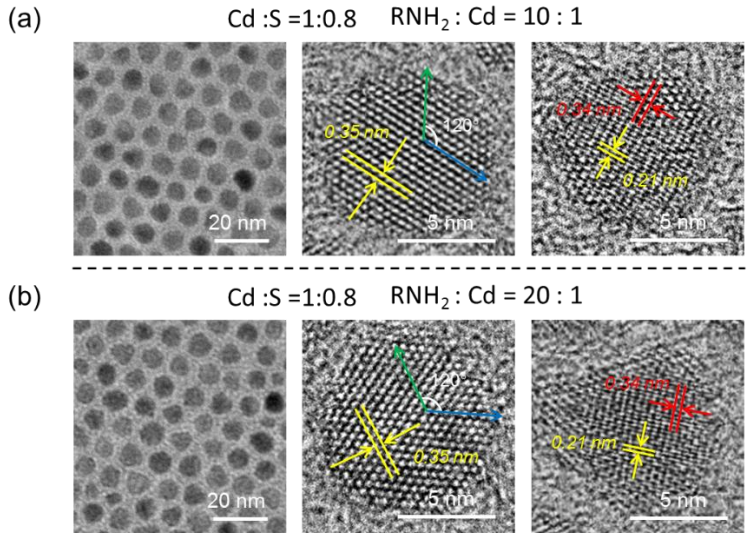

Figure S4. (a) TEM images and HRTEM images of the samples synthesized with Cd:S=5:4, RNH_2 : Cd = 10 : 1. (b) TEM images and HRTEM images of the samples synthesized with Cd:S=5:4, RNH_2 : Cd = 20 : 1. In both cases, all core/shell nanocrystals are with dot-shaped two-dimensional projection (left) . However, HRTEM images reveal that, in both cases, these dot-shaped two-dimensional projections of the core/shell nanocrystals can possess two types of orientations, i.e., with c-axis either perpendicular (middle) or parallel (right) to the electron beam.

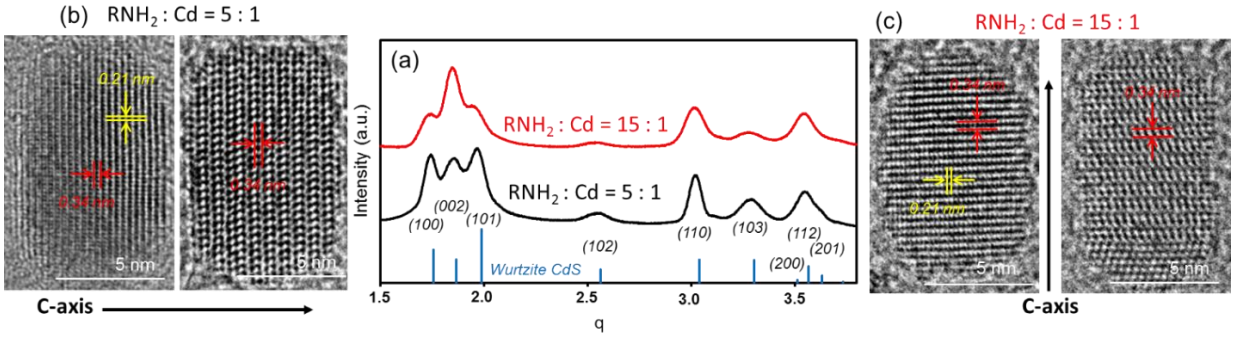

Figure S5. (a) XRD patterns of CdSe/CdS core/shell nanocrystals in Figure 3. By increasing the amine concentration, the (002) peak of the nanocrystals becomes sharp and narrow, which is a clear signature of elongation along the c-axis. [1] (b, c) Additional HRTEM images of the nanocrystals with different zone axes from those in Figure 3 for each sample, which are consistent with the XRD patterns.

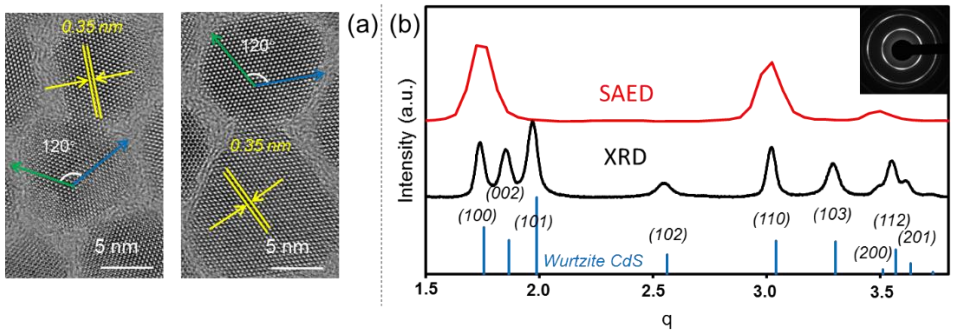

Figure S6. (a) High-resolution TEM images of the nanocrystals formed by oriented-attachment, which is the same reaction in Figure 3a (R'COOH : Cd = 5 : 1). Evidently, oriented-attachment occurs at the lateral facets, which results in the nanocrystals with large facets perpendicular to the c-axis and preferentially orient themselves on TEM substrates with their c-axis parallel to the electron beam. (b) XRD pattern (black) and integrated intensity profile from the SAED pattern (red) of the nanocrystals from the same reaction in Figure 3b (R'COOH : Cd = 12 : 1). Inset: The SAED pattern of the sample.

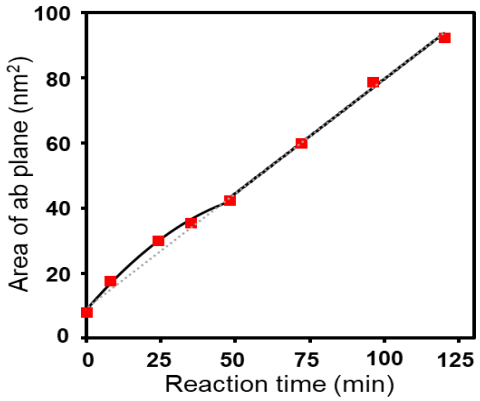

Figure S7. The average area of the two-dimensional projections of the nanocrystals deposited with a low-concentration solution versus the epitaxy time. The dotted line is the linear function for the epitaxial period after 48 minutes, indicating ideal two-dimensional growth. As expected, the early stage is super-linear, which leans toward three-dimensional growth. Simple geometric estimation would show that the area-growth rate would be inversely proportional to the growth time (equivalent to the amount of precursors).

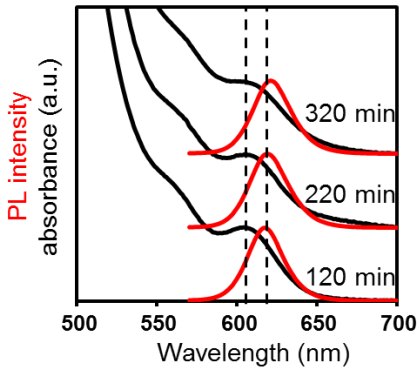

Figure S8. UV-Vis and PL spectra of the samples from 120 minutes to 320 minutes for the reaction related to Figures 5 and 6.

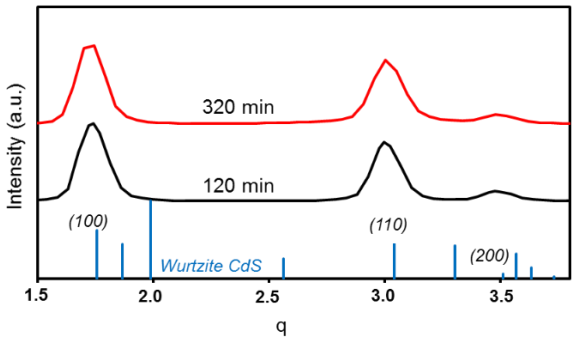

Figure S9. Integrated intensity profile for the SAED patterns of the CdSe/CdS core/shell nanocrystals at 120min and 320 minutes in Figure 6.

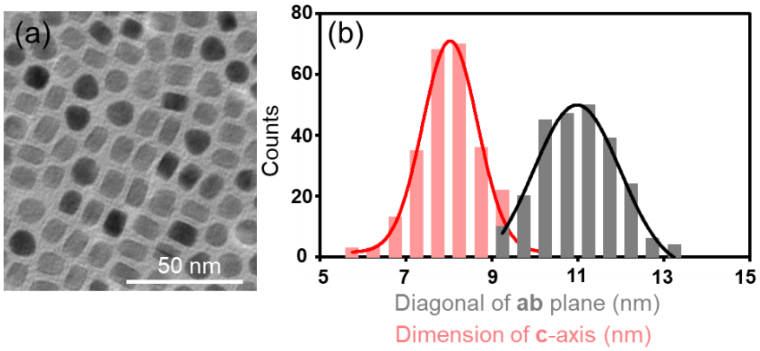

Figure S10. (a) TEM image and (b) the related statistic data of CdSe/CdS core/shell nanocrystals synthesized by increasing the primary amine concentration. In comparison with Figures 5 and 6, the only change of epitaxy conditions is to double the amine concentration, i.e., RNH_2 : Cd = 10 : 1.

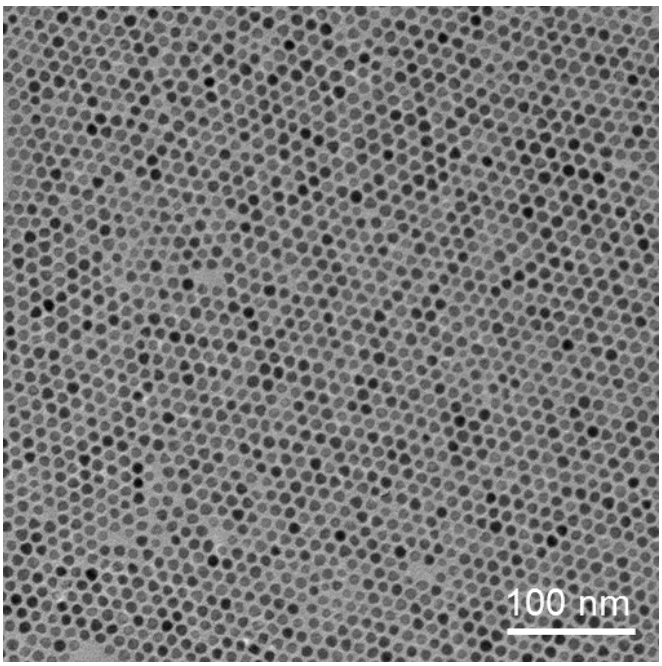

Figure S11. A large view of TEM images of the CdSe@CdS dot@nanoplatelet 2D nanocrystals with 6 nm in thickness and 10.6 nm in lateral dimension. Under the deposition conditions for the thin-film samples for measuring the polarized emission, nearly all 2D nanocrystals oriented themselves with their c-axis (thickness direction) perpendicular to the substrate.

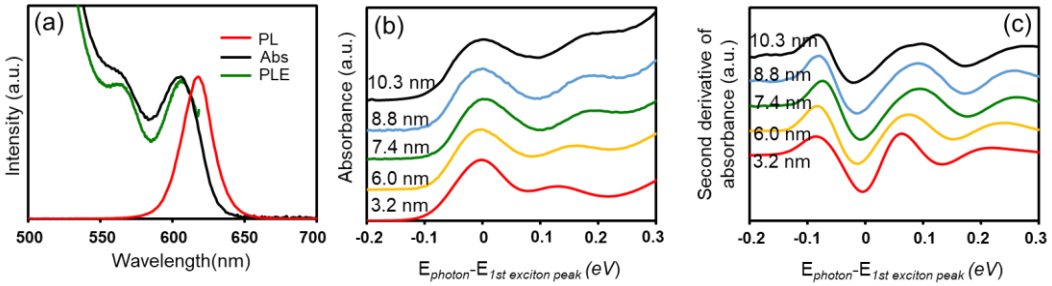

Figure S12. (a) UV-Vis, PL, and PLE spectra of the CdSe@CdS dot@nanoplatelet 2D nanocrystals. No sign of the splitting of the first excitonic absorption is observed. (b) Wavelength-adjusted UV-Vis spectra during the epitaxial growth of the 2D nanocrystals, which always shows a single peak for the first excitonic absorption. (c) Second derivatives of the wavelength-adjusted UV-Vis spectra during the epitaxial growth of the 2D nanocrystals, indicating no obvious splitting of the first excitonic absorption. The lateral dimension for each sample is provided for (b) and (c).

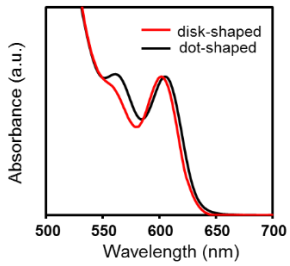

Figure S13. Comparison of UV-Vis spectra of dot-shaped and disk-shaped CdSe/CdS core/shell nanocrystals with similar absorption peak position. Evidently, the first excitonic absorption for two samples possesses nearly identical peak width and peak contour, implying no obvious splitting of the 2D nanocrystals.

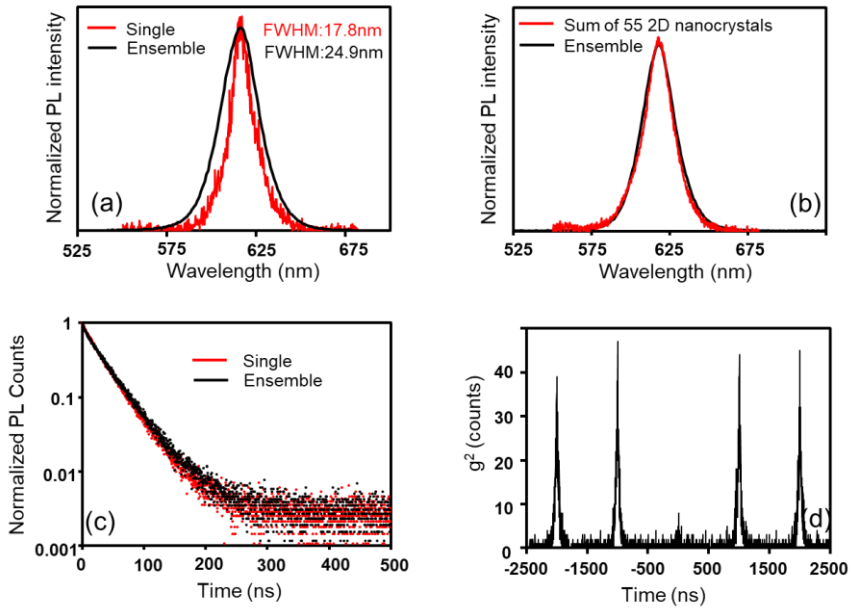

Figure S14. (a) PL spectra of ensemble and representative single 2D nanocrystal. (b) PL spectra of ensemble and sum of 55 2D nanocrystals. (c) PL decay dynamics of representative single 2D nanocrystal and ensemble nanocrystals in solution. (a) Second-order photon correlation of representative single 2D nanocrystal.

Reference:

(1) Peng, X.; Manna, L.; Yang, W.; Wickham, J.; Scher, E.; Kadavanich, A.; Alivisatos, A. P., Shape control of CdSe nanocrystals. *Nature* **2000,** *404*, 59-61.